









RESEARCH ARTICLE | NOVEMBER 16 2021

Metallic capped quasi-two-dimensional electron gas in a SrTiO₃-based heterostructure

Huichao Wang  ; Chun Hung Suen ; Hui Li ; Songhua Cai  ; Xiaoyuan Zhou ; Jiannong Wang  ; Ji-Yan Dai  

 Check for updates

Appl. Phys. Lett. 119, 201602 (2021)

<https://doi.org/10.1063/5.0074499>


View
Online


Export
Citation

CrossMark

starting at
EUR 6.360,-



Grows with your experiment.
The MFLI Lock-in Amplifier.

Field-upgradeable options

- 5 MHz frequency extension
- PID controller
- Multi-frequency analysis
- Impedance analyzer



[Find out more](#)

Metallic capped quasi-two-dimensional electron gas in a SrTiO₃-based heterostructure

Cite as: Appl. Phys. Lett. **119**, 201602 (2021); doi: [10.1063/5.0074499](https://doi.org/10.1063/5.0074499)

Submitted: 8 October 2021 · Accepted: 30 October 2021 ·

Published Online: 16 November 2021 · Corrected: 17 November 2021



View Online



Export Citation



CrossMark

Huichao Wang,^{1,a)} Chun Hung Suen,² Hui Li,³ Songhua Cai,^{2,a)} Xiaoyuan Zhou,⁴ Jiannong Wang,^{3,a)} and Ji-Yan Dai^{2,a)}

AFFILIATIONS

¹School of Physics, Sun Yat-Sen University, Guangzhou 510275, China

²Department of Applied Physics, The Hong Kong Polytechnic University, Hung Hom, Kowloon, Hong Kong, China

³Department of Physics, Hong Kong University of Science and Technology, Hong Kong, China

⁴College of Physics, Chongqing University, Chongqing 401331, China

^{a)}Authors to whom correspondence should be addressed: wanghch26@mail.sysu.edu.cn; songhua.cai@polyu.edu.hk; phjwang@ust.hk; and jijyan.dai@polyu.edu.hk

ABSTRACT

Two-dimensional electron gas (2DEG) in SrTiO₃ (STO)-based heterostructures has been a subject of intense scientific interest in recent years. In this work, the metallic transition metal dichalcogenides ZrTe₂ was grown on STO by pulsed laser deposition and AlN was subsequently deposited as a protection layer. The high-resolution transmission electron microscopy and electron energy loss spectroscopy results demonstrated the system as a multilayer structure of AlN/ZrTe₂/ZrO₂/STO due to interface redox reactions and implied a conductive STO surface. The remarkable Shubnikov–de Haas oscillations detected by angular dependent magnetotransport measurements reveal clear evidence of a high mobility quasi-2DEG in the STO-based interface. Moreover, evidence for extra carriers with three-dimensional features is observed implying the multiband contributions, which provide an explanation for some anomalous behavior in STO-based heterostructures. In addition, the thickness dependence study suggests the charge transfer effect between the capping metallic topological material ZrTe₂ and the interfacial 2DEG. This work provides insight into the intrinsic electronic structure of STO-based heterostructures, and the integrated systems can serve as a platform for studying the interplay of the 2DEG with attractive materials as well as developing practical device applications.

Published under an exclusive license by AIP Publishing. <https://doi.org/10.1063/5.0074499>

Heterostructures based on transition metal oxides are emerging as one of the most attractive systems in condensed matter physics due to the wide range of extraordinary properties.^{1–10} The intriguing quantum phenomena include the high mobility 2DEG, superconductivity, tunable Rashba spin–orbit interaction, ferromagnetism, giant thermoelectric effect, and quantum Hall effect, which are of great significance from both scientific and technological perspectives. In particular, the LaAlO₃/SrTiO₃ (LAO/STO) heterointerface has long been a focus in this field and was well-studied since the discovery of the high mobility 2DEG in 2004.¹ The conducting interface between these two insulating perovskites was demonstrated by various experimental probes, which include the electrical transport measurements, x-ray photoemission spectroscopy (XPS), high-resolution scanning/transmission electron microscopy (HRS/TEM) imaging with electron energy loss spectroscopy (EELS), and x-ray absorption spectroscopy (XAS). Particularly, the quantum oscillations, e.g., the Shubnikov–de Haas (SdH) effect,

have been a powerful tool to demonstrate the formation of the 2DEG and shed light on the intrinsic electronic structure of the heterostructures.^{11–24} However, some open questions remain. For instance, the origin of the interface conductivity is still controversial in spite of some prevailing mechanisms, including the polar discontinuity, cation exchange, and the formation of oxygen vacancies. In addition, different frameworks are proposed to explain the discrepancy between the concentration extracted from SdH oscillations and that determined by the Hall traces.

Creating similar conducting heterointerfaces based on STO can be a useful way to deeply understand the electron gas between the insulating oxide materials and open prospects of functionalities of the 2DEG. The formation of a conductive interface was later revealed in many other transition metal oxides,^{10–29} especially the STO-based heterostructures, such as γ -Al₂O₃/STO,¹⁵ LaTiO₃/STO,^{21,23} and CaZrO₃/STO.²⁹ Note that both crystalline and amorphous top layers work for

the appearance of the 2DEG in spite of the different physical origins. Since the conducting electrons are always confined in the STO surface associated with the Ti 3d subbands, the various systems show some consistent characteristics for the interface carriers. Moreover, it is found that different top layers generate much more fruitful physics and functionality. For example, the γ -Al₂O₃/SrTiO₃ heterostructure exhibits the highest carrier mobility exceeding 100 000 cm² V⁻¹ s⁻¹ at 2 K;¹⁵ CaZrO₃/STO shows strain induced polarization and results in a high mobility 2DEG;²⁹ the amorphous LAO/STO demonstrates the oxygen vacancies as the charge source.³⁰ In addition, the electronic transport properties of the STO-based heterointerface are very sensitive and can be modulated by a spacing layer,⁷ a capping layer, or surface treatment through chemical and electrostatic effects.^{31–39} For instance, the critical thickness in LAO/STO can be tuned down via the Co or Al metal capping layer through transfer of charges to the interface.^{35,36} Pt/LAO/STO shows nonvolatile resistive switching acting as a memory device.³³ Thus, the quasi-2DEG in other STO-based heterostructures and its integration with attractive materials due to the rich properties and the great promise in applications deserve more study.

The motivation of designing the ZrTe₂/STO structure is trying to probe the possible coupling between STO and the topological material ZrTe₂, while unexpectedly, an interfacial reaction induces the formation of the Te doped ZrO₂/STO interface characterized by the HRS/TEM and EELS results. The hybrid heterostructure shows remarkable SdH effects arising from the high mobility quasi-2DEG in the STO-based interface. Moreover, we observe evidence for the coexisting three-dimensional (3D) carriers as a support for the multiband mechanism. In addition, the charge transfer effect between the capping metallic topological material ZrTe₂ and the interfacial quasi-2DEG was revealed by the results of the systems with different ZrTe₂ thicknesses. The work provides insights into the intrinsic electronic structure of the STO-based interface, and the high mobility 2DEG in the metallic capped oxide heterostructures can be promising platforms for electronic applications.

As reported in an earlier work,⁴⁰ we deposited the Zr–Te compound on the insulating (110) STO substrates for the formation of topological ZrTe₂ thin films. The laser source was a KrF excimer laser with a wavelength of 248 nm. The substrate-target distance during the deposition was 5 cm with the base pressure of around 5×10^{-5} Pa, and the films were grown at an optimized substrate temperature (T_s) of 550 °C. Since ZrTe₂ is sensitive to air, an additional amorphous AlN layer was deposited at 200 °C on top for protection with a thickness of about 70 nm. A 16T-PPMS (physical properties measurement system) was utilized for the magnetotransport measurements here. The electrodes are made via ultrasonic bonding with Al wires. Before the electron transport measurements in the PPMS, the samples were always kept at vacuum conditions.

Figure 1(a) shows the normalized magnetoresistance (MR) of the 70 nm thick ZrTe₂ on STO subject to a perpendicular magnetic field. Remarkably, quantum oscillations were observed to be superimposed on a background of the large positive MR at low temperatures below 4 K. Figure 1(b) shows the oscillations after subtracting a smooth polynomial background from the measured MR. The periodicity in the reciprocal of the magnetic field (1/B) demonstrates the SdH effect as the underlying origin. It is known that the SdH effect is a useful tool to detect intrinsic information of the

electronic structure of solids. The Landau fan diagram shown in Fig. 1(c) confirms the periodicity in 1/B of the oscillations. Linear fit gives a slope of 0.034, corresponding to a characteristic oscillating frequency of 29.4 T. The fast Fourier transform (FFT) results further reveal that the frequency peak is about 29.5 T as shown in Fig. 1(d), consistent with the linear fit results. The SdH oscillation amplitude follows the Lifshitz–Kosevich formula as¹⁹

$$\Delta R_{xx} \propto \exp(-2\pi^2 k_B T_D / \hbar \omega_c) \frac{2\pi^2 k_B T / \hbar \omega_c}{\sinh(2\pi^2 k_B T / \hbar \omega_c)},$$

where ΔR_{xx} is the oscillatory component of the resistance, ω_c is the cyclotron frequency (eB/m*), k_B is Boltzmann's constant, and \hbar is Planck's constant divided by 2π . Thus, the carrier effective mass can be extracted by analyzing the temperature dependence of the oscillations with $\Delta R_{xx}(T) \propto \lambda(T)/\sinh\lambda(T)$ and the factor $\lambda(T) = 2\pi^2 k_B T m^* / \hbar e B$. We chose five fixed magnetic field values showing oscillation peaks or dips and fit the oscillatory amplitude. The cyclotron effective mass is estimated to be $m^* = 1.3 m_0$ with m_0 representing the bare electron mass. In addition, the Dingle temperature T_D is deduced from the slope of the Dingle plot, i.e., $\ln[\Delta R_{xx} B \sinh \lambda(T)]$ vs 1/B. The fitting of measured quantum oscillations gives a $T_D = 1.3$ K [Fig. 1(f)], corresponding to a quantum scattering time of $\tau_q = \hbar / 2\pi k_B T_D = 1.0$ ps. According to the relation $\mu = e\tau/m^*$, the quantum mobility $\mu_{SdH} = 1.3 \times 10^3$ cm² V⁻¹ s⁻¹.

The magnetic field orientation dependence of the quantum oscillations is shown in Fig. 2(a). The angle between the external magnetic field and the normal direction of the film plane is defined as θ . Thus, the $\theta = 0^\circ$ indicates a perpendicular field and $\theta = 90^\circ$ denotes a parallel configuration of the electrical and magnetic fields. Figure 2(b) shows the first derivative dR_{xx}/dB for the measured raw data in Fig. 2(a), and Fig. 2(c) shows the oscillations vs the perpendicular component B_\perp . We can see that the oscillations are only dependent on the perpendicular field $B \cos\theta$ in a small θ regime $\theta < 26^\circ$. This is consistent with Fig. 2(d) showing the peak/dip positions for $\theta < 26^\circ$ can be reproduced by a $\cos\theta$ fit. Thus, these results illustrate the appearance of the quasi-2DEG in the system.

According to Luttinger's theorem,¹² $n_{2D} = N_v N_s e F / h$, where N_v is the valley degeneracy, N_s is the spin degeneracy, e is the elementary charge, F is the oscillating frequency, and h is Planck's constant. We calculated $n_{2D} = 1.4 \times 10^{12}$ cm⁻² with the choice of $N_v = 1$ and $N_s = 2$. Assuming the carriers are from the 70 nm thick ZrTe₂, a 3D carrier density $n_{2D} = 2.0 \times 10^{17}$ cm⁻³ was obtained, which is three orders of magnitude smaller than that from the Hall analysis.⁴⁰ In addition, it is noted that the effective mass obtained from the quantum oscillations is much larger than expected for a topological material with massless or massive Dirac fermions. The layered transition metal dichalcogenides (TMDCs) ZrTe₂ has attracted attention as a potential topological Dirac semimetal candidate.^{41–43} The angle-resolved photoemission spectroscopy experiments reveal a much smaller effective mass of 0.7 m_0 or 0.18 m_0 in ZrTe₂.⁴¹ The inconsistencies suggest that the quantum oscillations may not arise from ZrTe₂ and the origin needs to be further understood. In fact, it is found that the effective mass of 1.3 m_0 well matches with most results acquired in conductive STO surfaces.^{13–21} Considering the possibility of interface redox reactions when depositing ZrTe₂ on STO, the STO substrate may be reduced due to the formation of oxygen vacancies, and the interfacial

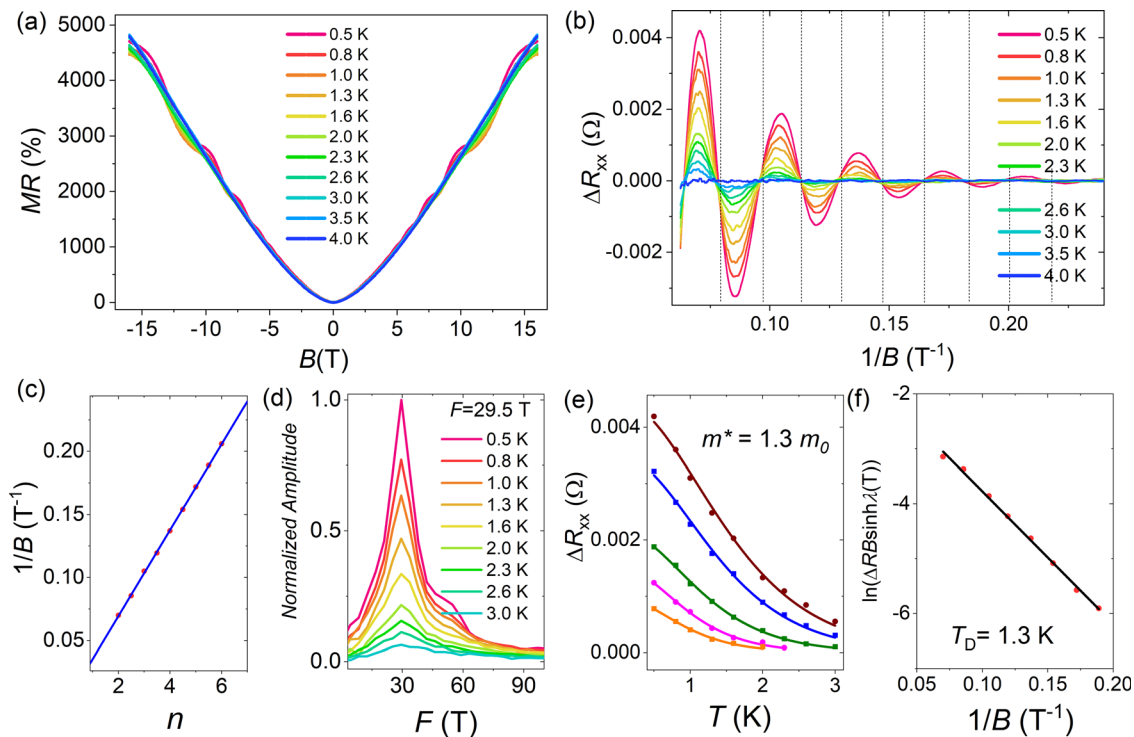


FIG. 1. SdH oscillations in the STO-based heterostructure. (a) Normalized MR of the heterostructure at selected low temperatures. (b) Extracted oscillatory components from the raw MR results in (a). (c) Landau fan diagram for the SdH oscillations at 0.5 K. (d) Normalized fast Fourier transform results for the MR oscillations in (b). (e) SdH oscillation amplitude extracted from (b) as a function of temperature at different magnetic fields. Solid lines are fit by the Lifshitz-Kosevich formula. (f) Dingle plots of $\ln[\Delta R(B, T)B \sinh \lambda(T)]$ vs $1/B$. A Dingle temperature of 1.3 K is obtained, corresponding to a quantum scattering time of $\tau_q \sim 1.0$ ps and a quantum mobility of about $1300 \text{ cm}^2 \text{ V}^{-1} \text{ s}^{-1}$.

effect can, thus, play a significant role in the observed exotic transport properties.

To determine the origin of the oscillations, the multilayer structure was examined carefully by HRS/TEM. HRTEM images were acquired on a JEOL 2100F TEM, operated at 200 kV. Scanning TEM (STEM) images were acquired on a Thermofisher Titan G2 60–300 aberration corrected STEM. The accelerating voltage of an electron beam is 300 kV. The convergence angle of an electron probe for STEM-HAADF imaging is 22.5 mrad, and the collection angle of an annular detector is 79.5–200 mrad. The cross-sectional HRSTEM image of the sample is shown in Fig. 3(a). One can see that a layered structure occupies the major part of the deposited film. The layer spacing is well consistent with the lattice constant $c = 0.66 \text{ nm}$ of ZrTe_2 . The 1T- ZrTe_2 has a hexagonal close-packed crystal structure. A unit cell of ZrTe_2 is denoted by a rectangle in Fig. 3(b) and can also be identified in the magnified HRSTEM image. It is worth noting that between the layered ZrTe_2 and the STO substrate, there exists a $\sim 15 \text{ nm}$ thick interfacial layer with different lattice structure with ZrTe_2 . A detailed analysis of the lattice spacing and their angles suggests that this interfacial layer belongs to ZrO_2 . The HRS/TEM results clearly confirm the interfacial reaction between the deposited ZrTe_2 and the STO substrate.

STEM energy dispersive x-ray (EDX) spectroscopy element mapping and the EELS study are further performed to characterize the interfacial region. As shown in Fig. 4(a), the EDX mapping results

reveal that the distributions of O and Te are not uniform along the thickness direction. In particular, the signal intensity of O decreases near the interface compared to the signal for the substrate underneath. It is surprising to see that O even exists in the whole film, suggesting an out diffusion of O from STO, which can be proven by EELS line-scan analysis across the interface as shown in Figs. 4(b) and 4(c). By extracting the signals of Ti and O edges from the EELS spectrum, the energy loss near edge structures reveals that the four unit cells of STO from the interface exhibit a different chemical state with bulk STO. From the fourth layer of STO up to the interfacial layer, the valence state of Ti cations degrades from Ti^{4+} to Ti^{3+} (peak shift and shape variation in Fig. 4(b) with a corresponding change in the O k-edge fine structure [Fig. 4(c)]. The interfacial characteristics imply a conductive STO surface, which is analogous to the similar situation in the oxide heterostructures such as LAO/STO cases. It is noted that a small Te peak can also be seen near the STO surface [Fig. 4(a)], so the interfacial layer is Te Doped ZrO_2 .

We point out that the interfacial effects mainly arising from the redox reactions and the caused quasi-2DEG due to oxygen vacancies should not be related to the orientation of the STO substrate. In the previous report, the HRTEM images of the system on (110) STO also reveal a 5 nm thick interfacial layer presenting a different layer spacing,⁴⁰ which is consistent with the presented HRTEM results here on (100) STO. The interfacial layer ZrO_2 implies the chemical reactions in the interface. Thus, the observation of the quasi-2DEG can be

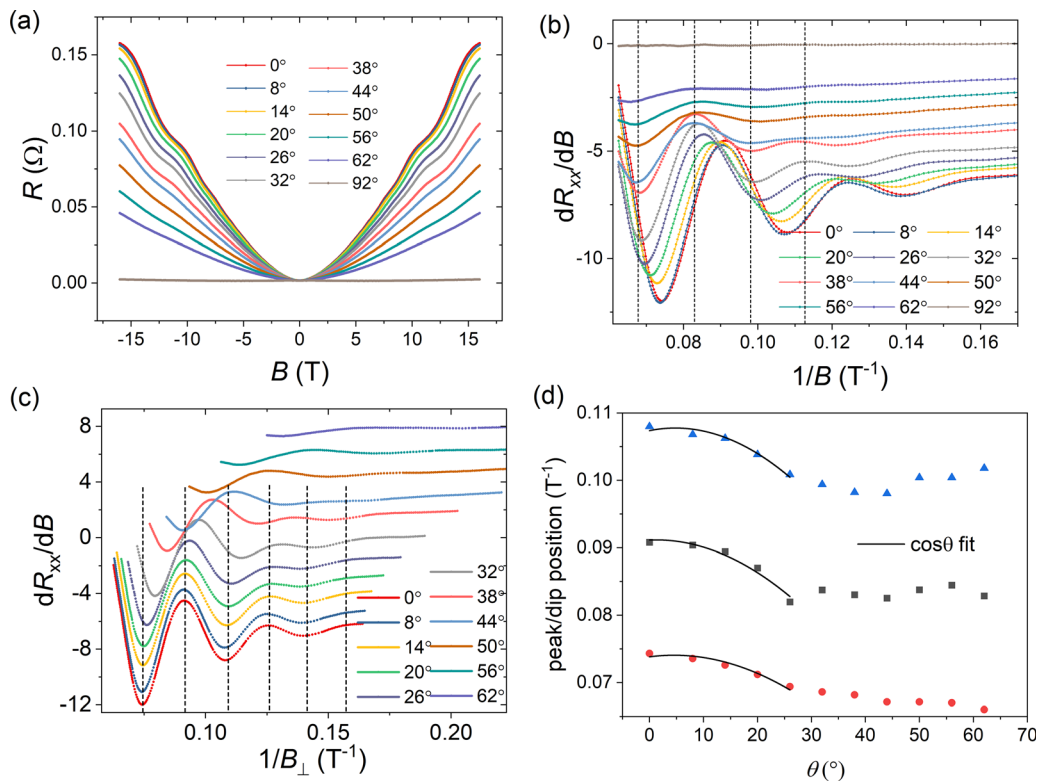


FIG. 2. Magnetic field orientation dependence of the SdH oscillations in the STO-based heterostructure. (a) MR as a function of the magnetic field measured at varying tilted angles θ . The angle 0° indicates a field perpendicular to the film plane and 90° denotes a parallel configuration of the electrical and magnetic fields. (b) The first derivative (dR_{xx}/dB) for the raw MR data in (a). (c) Quantum oscillations as a function of the perpendicular component B_\perp of the external magnetic fields. (d) Angular dependence of the peak/dip positions in dR_{xx}/dB . The black curves denote the fit by $A \cos \theta$ with A being a parameter.

attributed to the corresponding oxygen vacancies in the reduced (110) STO. Accordingly, based on the HRS/TEM and EELS results of the system on the (100) STO, it is credible that the conductive STO surface hosts the quasi-2DEG analogous to the situation in most STO-based heterostructures.

Thus, we demonstrate the formation of the high mobility 2DEG in the AlN/ZrTe₂/ZrO₂/STO integrated system, which closely related to the interface redox reactions.²⁸ Our previous study has revealed a quasi-2D transport characteristic of the STO-based heterostructure.⁴⁰ The quasi-2D transport feature is consistent with the layered structure

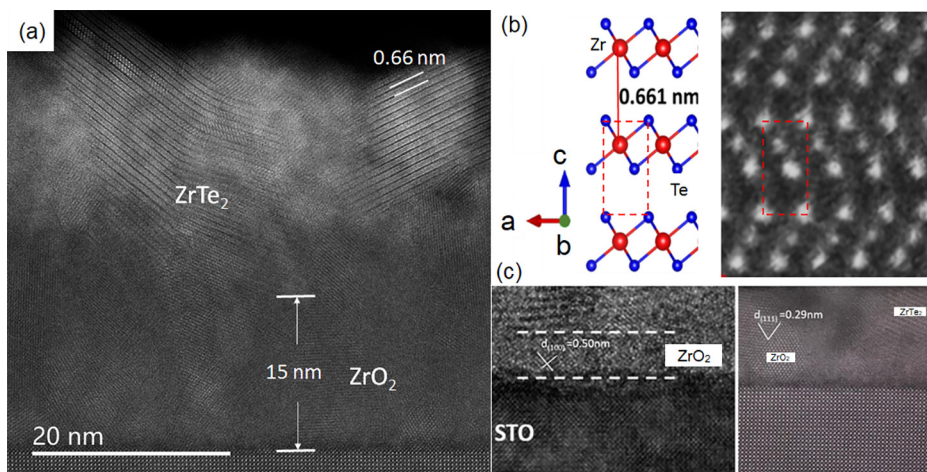


FIG. 3. Heterointerface characterization by HRTEM and STEM. (a) HRSTEM image of the multilayer structure, where an interfacial layer can be identified between the STO substrate and the ZrTe₂ film. (b) Magnified image showing the correspondence of real unit cell (marked by a red rectangle) with the crystal structure model of ZrTe₂. (c) HRTEM and STEM image of the interfacial structure identified as ZrO₂.

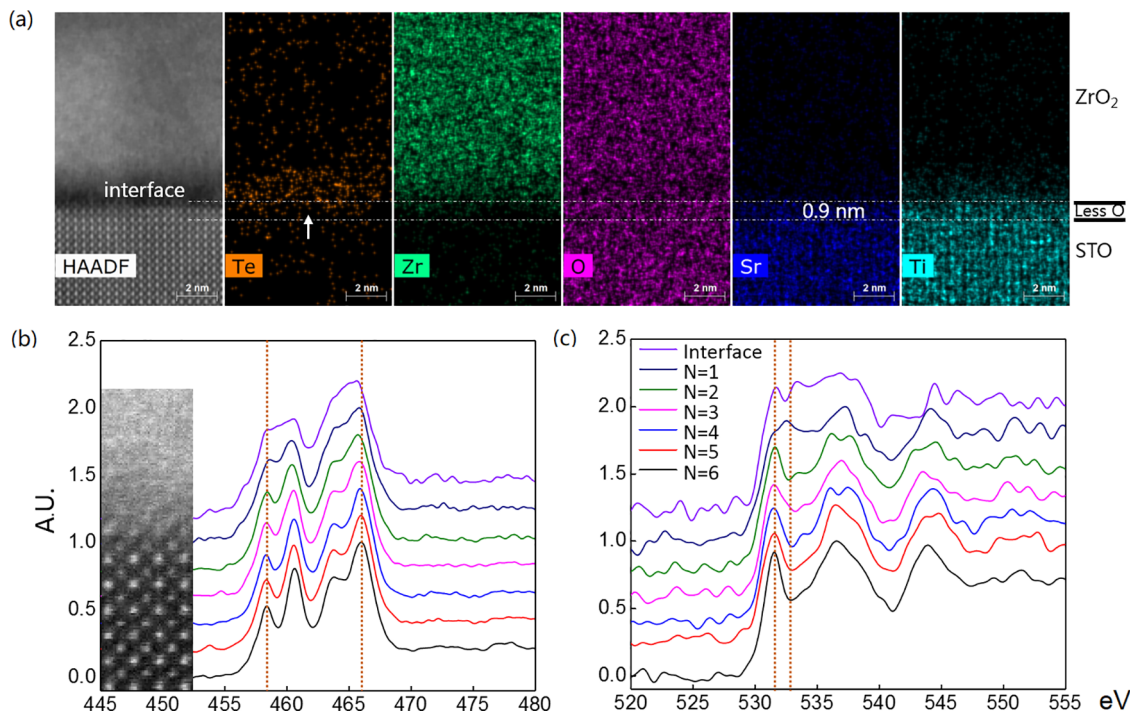


FIG. 4. Elemental mapping and interfacial valence states of Ti and O ions. (a) STEM-EDS element mapping across the interface. (b) EELS results of Ti 3d L-edge shift peaks and (c) O 2p K-edge fine structure across the interface.

of ZrTe₂. However, the study reveals that the STO-interface is conducting and the interfacial quasi-2DEG may play a significant role for the exotic transport properties. It is noted that our control experiments reveal that STO dealt with the same low oxygen pressure and the high temperature process without any capping materials is highly insulating. So the conductivity from bulk STO can be excluded. However, the deposition of compounds induces an interfacial reaction and reduces STO contributing to the electron transport. A reference sample was prepared with the structure of ZrTe₂/ZrO₂/STO without the protection layer, and it becomes insulating soon when exposure to air. The oxidation of ZrTe₂ itself cannot explain the metal-insulator transition of the interface. We attribute it to the filling of the oxygen vacancies, origin of the conductive interface, into the STO substrate in the air. The mechanism is well consistent with previous studies.⁴⁴

In addition, it is found that the electric conductivity of the multilayer system is thickness dependent. For a thinner ZrTe₂ film above the ZrO₂/STO heterointerface, the system shows larger sheet resistance. Meanwhile, the EELS results show that the signal of Ti³⁺ at the interfacial region is weak. In addition, the control sample of the ZrTe₂ thin film grown on Al₂O₃ reveals that ZrTe₂ itself is also more resistive than the AlN/ZrTe₂/ZrO₂/STO system. The results indicate that the metallic ZrTe₂ film above the conducting ZrO₂/STO interface actually enhances the total conductivity. As reported, the capping metallic layer can dramatically modify the electronic response of LAO/STO interfaces. For example, the Co or Al cap layer makes the 2DEG in LAO/STO more conducting.^{35,36} As known, electrons in a heterostructure would transfer to the material with the larger work function until the equilibrium when the Fermi levels of both sides align together. The

larger conductance in the metallic capped 2DEG system may be attributed to similar charge transfer effects between the interface and the metallic ZrTe₂ films.

Finally, we want to recall Fig. 2(b), in which we can see magnetic field orientation independent SdH oscillations for larger angles $\theta > 44^\circ$. This suggests a coexistence of carriers with 3D nature and the quasi-2DEG. The features have never been observed in STO-based heterostructures as a direct evidence for proposed multiband contributions.^{15,17,19,22} In fact, the Ti d_{xy} band features the 3D characteristic extending deep into STO as predicted, and the hybridization of $d_{xz/yz}$ bands contributes to the 2D nature due to the anisotropy.²³ The multiband framework could explain some anomalous behaviors in STO-heterostructures such as the discrepancy of carrier densities inferred from the SdH oscillations and the Hall traces²⁵ and the phase shift of quantum oscillations in large tilted angles.¹⁵ Moreover, the observation of the coexisted 2D or 3D features in the system may shed light on the observation of different 2D or 3D characters for the conducting carriers in the STO-based interface.^{12–23} Thus, these results provide insight into the deep understanding of the general STO-based heterostructures considering that the conducting electrons are always confined in the SrTiO₃ surface.

In summary, we report the observation of the high mobility quasi-2DEG in the multilayer structure of AlN/ZrTe₂/ZrO₂/STO characterized by the HRS/TEM and EELS results. The conspicuous SdH oscillations reveal the coexistence of carriers with 3D nature and the quasi-2DEG showing $\cos \theta$ dependence on the magnetic field, which provides clear evidence for the multiband contribution in the STO-interface and explains some anomalous behaviors in similar oxide

heterostructures. The metallic capped ZrTe₂ further enhances the conductivity of the system, which integrates the topological material and the quasi-2DEG in the STO-interface. This work provides insight into the intrinsic properties of STO-based heterostructures and paves way for the design of high-mobility oxide electronics.

We thank support from the National Natural Science Foundation of China (Grant Nos. 12004441, 11674040, and 11904039), the Fundamental Research Funds for the Central Universities (Grant Nos. 2018CDQYWL0048, 106112017CDJQJ308821, and 2018CDPTCG0001/26), and the Hong Kong Polytechnic University (Grant Nos. 1-ZVSQ, UAEZ, 4-ZZDC, and DD7F). H.W. acknowledges the support of the Hundreds of Talents program of Sun Yat-Sen University and the Fundamental Research Funds for the Central Universities (No. 2021qntd27). S.C. acknowledges the support of a startup grant from the Hong Kong Polytechnic University (No. 1-BQ96); the General Research Fund (Nos. 15306021 and 16301418) from the Hong Kong Research Grant Council; and the open subject of National Laboratory of Solid State Microstructures, Nanjing University (No. M34001).

AUTHOR DECLARATIONS

Conflict of Interest

The authors have no conflicts to disclose.

Author Contributions

H.W., C.H.S., and H.L. contributed equally to this work.

DATA AVAILABILITY

The data that support the findings of this study are available from the corresponding authors upon reasonable request.

REFERENCES

- A. Ohtomo and H. Y. Hwang, "A high-mobility electron gas at the LaAlO₃/SrTiO₃ heterointerface," *Nature* **427**, 423 (2004).
- N. Reyren, S. Thiel, A. D. Caviglia, L. Fitting Kourkoutis, G. Hammerl, C. Richter, C. W. Schneider, T. Kopp, A.-S. Rüetsch, D. Jaccard, M. Gabay, D. A. Muller, J.-M. Triscone, and J. Mannhart, "Superconducting interfaces between insulating oxides," *Science* **317**, 1196 (2007).
- A. Brinkman, M. Huijben, M. van Zalk, J. Huijben, U. Zeitler, J. C. Maan, W. G. van der Wiel, G. Rijnders, D. H. A. Blank, and H. Hilgenkamp, "Magnetic effects at the interface between non-magnetic oxides," *Nat. Mater.* **6**, 493–496 (2007).
- A. D. Caviglia, S. Gariglio, N. Reyren, D. Jaccard, T. Schneider, M. Gabay, S. Thiel, G. Hammerl, J. Mannhart, and J.-M. Triscone, "Electric field control of the LaAlO₃/SrTiO₃ interface ground state," *Nature* **456**, 624 (2008).
- J. A. Bert, B. Kalisky, C. Bell, M. Kim, Y. Hikita, H. Y. Hwang, and K. A. Moler, "Direct imaging of the coexistence of ferromagnetism and superconductivity at the LaAlO₃/SrTiO₃ interface," *Nat. Phys.* **7**, 767 (2011).
- L. Li, C. Richter, J. Mannhart, and R. C. Ashoori, "Coexistence of magnetic order and two-dimensional superconductivity at LaAlO₃/SrTiO₃ interfaces," *Nat. Phys.* **7**, 762–766 (2011).
- Y. Z. Chen, F. Trier, T. Wijnands, R. J. Green, N. Gauquelin, R. Egoavil, D. V. Christensen, G. Koster, M. Huijben, N. Bovet, S. Macke, F. He, R. Sutarro, N. H. Andersen, J. A. Sulpizio, M. Honig, G. E. Prawiroatmodjo, T. S. Jespersen, S. Linderroth, S. Ilani, J. Verbeeck, G. Van Tendeloo, G. Rijnders, G. A. Sawatzky, and N. Pryds, "Extreme mobility enhancement of two-dimensional electron gases at oxide interfaces by charge-transfer-induced modulation doping," *Nat. Mater.* **14**, 801 (2015).
- Y. Lei, Y. Li, Y. Z. Chen, Y. W. Xie, Y. S. Chen, S. H. Wang, J. Wang, B. G. Shen, N. Pryds, H. Y. Hwang, and J. R. Sun, "Visible-light-enhanced gating effect at the LaAlO₃/SrTiO₃ interface," *Nat. Commun.* **5**, 5554 (2014).
- D. V. Christensen, F. Trier, W. Niu, Y. Gan, Y. Zhang, T. S. Jespersen, Y. Chen, and N. Pryds, "Stimulating oxide heterostructures: A review on controlling SrTiO₃-based heterointerfaces with external stimuli," *Adv. Mater. Interfaces* **6**, 1900772 (2019).
- Y. Chen and R. J. Green, "Progress and perspectives of atomically engineered perovskite oxide interfaces for electronics and electrocatalysts," *Adv. Mater. Interfaces* **6**, 1900547 (2019).
- Y. Kozuka, M. Kim, C. Bell, B. G. Kim, Y. Hikita, and H. Y. Hwang, "Two-dimensional normal-state quantum oscillations in a superconducting heterostructure," *Nature* **462**, 487 (2009).
- M. Ben Shalom, A. Ron, A. Pavevski, and Y. Dagan, "Shubnikov–De Haas oscillations in SrTiO₃/LaAlO₃ interface," *Phys. Rev. Lett.* **105**, 206401 (2010).
- A. D. Caviglia, S. Gariglio, C. Cancellieri, B. Sacépé, A. Fête, N. Reyren, M. Gabay, A. F. Morpurgo, and J.-M. Triscone, "Two-dimensional quantum oscillations of the conductance at LaAlO₃/SrTiO₃ interfaces," *Phys. Rev. Lett.* **105**, 236802 (2010).
- P. Moetafeg, D. G. Ouellette, J. R. Williams, S. J. Allen, L. Balents, D. G. Gordon, and S. Stemmer, "Quantum oscillations from a two-dimensional electron gas at a Mott/band insulator interface," *Appl. Phys. Lett.* **101**, 151604 (2012).
- Y. Z. Chen, N. Bovet, F. Trier, D. V. Christensen, F. M. Qu, N. H. Andersen, T. Kasama, W. Zhang, R. Giraud, J. Dufouleur, T. S. Jespersen, J. R. Sun, A. Smith, J. Nygard, L. Lu, B. Buchner, B. G. Shen, S. Linderroth, and N. Pryds, "A high-mobility two-dimensional electron gas at the spinel/perovskite interface of γ -Al₂O₃/SrTiO₃," *Nat. Commun.* **4**, 1371 (2013).
- A. Fête, S. Gariglio, C. Berthod, D. Li, D. Stornaiuolo, M. Gabay, and J.-M. Triscone, "Large modulation of the Shubnikov–de Haas oscillations by the Rashba interaction at the LaAlO₃/SrTiO₃ interface," *New J. Phys.* **16**, 112002 (2014).
- A. McCollam, A. S. Wenderich, M. K. Kruize, V. K. Guduru, H. J. A. Molegraaf, M. Huijben, G. Koster, D. H. A. Blank, G. Rijnders, A. Brinkman, H. Hilgenkamp, U. Zeitler, and J. C. Maan, "Quantum oscillations and subband properties of the two-dimensional electron gas at the LaAlO₃/SrTiO₃ interface," *APL Mater.* **2**, 022102 (2014).
- Y. Xie, C. Bell, M. Kim, H. Inoue, Y. Hikita, and H. Y. Hwang, "Quantum longitudinal and Hall transport at the LaAlO₃/SrTiO₃ interface at low electron densities," *Solid State Commun.* **197**, 25–29 (2014).
- M. Yang, K. Han, O. Torresin, M. Pierre, S. W. Zeng, Z. Huang, V. Venkatesan, M. Goiran, J. M. D. Coey, Ariando, and W. Escoffier, "High field magnetotransport in two-dimensional electron gas LaAlO₃/SrTiO₃," *Appl. Phys. Lett.* **109**, 122106 (2016).
- F. Trier, G. E. D. K. Prawiroatmodjo, Z. C. Zhong, D. V. Christensen, M. V. Soosten, A. Bhowmik, J. M. G. Lastra, Y. Z. Chen, T. S. Jespersen, and N. Pryds, "Quantization of Hall resistance at the metallic interface between an oxide insulator and SrTiO₃," *Phys. Rev. Lett.* **117**, 096804 (2016).
- M. J. Veit, R. Arras, B. J. Ramshaw, R. Pentcheva, and Y. Suzuki, "Nonzero Berry phase in quantum oscillations from giant Rashba-type spin splitting in LaTiO₃/SrTiO₃ heterostructures," *Nat. Commun.* **9**, 1458 (2018).
- S. Zeng, W. Lü, Z. Huang, Z. Liu, K. Han, K. Gopinadhan, C. Li, R. Guo, W. Zhou, H. H. Ma, L. Jian, T. Venkatesan, and Ariando, "Liquid-gated high mobility and quantum oscillation of the two-dimensional electron gas at an oxide interface," *ACS Nano* **10**, 4532–4537 (2016).
- M. J. Veit, M. K. Chan, B. J. Ramshaw, R. Arras, R. Pentcheva, and Y. Suzuki, "Three-dimensional character of the Fermi surface in ultrathin LaTiO₃/SrTiO₃ heterostructures," *Phys. Rev. B* **99**, 115126 (2019).
- K. Rubi, J. Gosteau, R. Serra, K. Han, S. Zeng, Z. Huang, B. Warot-Fonrose, R. Arras, E. Snoeck, Ariando, M. Goiran, and W. Escoffier, "Aperiodic quantum oscillations in the two-dimensional electron gas at the LaAlO₃/SrTiO₃ interface," *npj Quantum Mater.* **5**, 9 (2020).
- G. Cheng, A. Annadi, S. Lu, H. Lee, J. W. Lee, M. Huang, C. B. Eom, P. Irvin, and J. Levy, "Shubnikov–de Haas-like quantum oscillations in artificial one-dimensional LaAlO₃/SrTiO₃ electron channels," *Phys. Rev. Lett.* **120**, 076801 (2018).
- P. Perna, D. Maccariello, M. Radovic, U. Scotti di Uccio, I. Pallecchi, M. Coddà, D. Marré, C. Cantoni, J. Gazquez, M. Varela, S. J. Pennycook, and F. Miletto Granozio, "Conducting interfaces between band insulating oxides: The LaGaO₃/SrTiO₃ heterostructure," *Appl. Phys. Lett.* **97**, 152111 (2010).

- ²⁷J. Biscaras, N. Bergeal, A. Kushwaha, T. Wolf, A. Rastogi, R. C. Budhani, and J. Lesueur, "Two-dimensional superconductivity at a mott insulator/band insulator interface LaTiO₃/SrTiO₃," *Nat. Commun.* **1**, 89 (2010).
- ²⁸Y. Z. Chen, N. Pryds, J. E. Kleibecker, J. R. Sun, E. Stamate, G. Koster, B. G. Shen, G. Rijnders, and S. Linderoth, "Metallic and insulating interfaces of amorphous SrTiO₃-based oxide heterostructures," *Nano Lett.* **11**, 3774 (2011).
- ²⁹Y. Z. Chen, F. Trier, T. Kasama, D. V. Christensen, N. Bovet, Z. I. Balogh, H. Li, K. Thyden, W. Zhang, S. Yazdi, P. Norby, N. Pryds, and S. Linderoth, "Creation of high mobility two-dimensional electron gases via strain induced polarization at an otherwise nonpolar complex oxide interface," *Nano Lett.* **15**, 1849 (2015).
- ³⁰Z. Q. Liu, C. J. Li, W. M. Lu, X. H. Huang, Z. Huang, S. W. Zeng, X. P. Qiu, L. S. Huang, A. Annadi, J. S. Chen, J. M. D. Coey, T. Venkatesan, and Ariando, "Origin of the two-dimensional electron gas at LaAlO₃/SrTiO₃ interfaces: The role of oxygen vacancies and electronic reconstruction," *Phys. Rev. X* **3**, 021010 (2013).
- ³¹R. Pentcheva, M. Huijben, K. Otte, W. E. Pickett, J. E. Kleibecker, J. Huijben, H. Boschker, D. Kockmann, W. Siemons, G. Koster, H. J. W. Zandvliet, G. Rijnders, D. H. A. Blank, H. Hilgenkamp, and A. Brinkman, "Parallel electron-hole bilayer conductivity from electronic interface reconstruction," *Phys. Rev. Lett.* **104**, 166804 (2010).
- ³²R. Arras, V. G. Ruiz, W. E. Pickett, and R. Pentcheva, "Tuning the two-dimensional electron gas at the LaAlO₃/SrTiO₃(001) interface by metallic contacts," *Phys. Rev. B* **85**, 125404 (2012).
- ³³S. Wu, X. Luo, S. Turner, H. Peng, W. Lin, J. Ding, A. David, B. Wang, G. V. Tendeloo, J. Wang, and T. Wu, "Nonvolatile resistive switching in Pt/LaAlO₃/SrTiO₃ heterostructures," *Phys. Rev. X* **3**, 041027 (2013).
- ³⁴Y. J. Shi, S. Wang, Y. Zhou, H. F. Ding, and D. Wu, "Tuning the carrier density of LaAlO₃/SrTiO₃ interfaces by capping La_{1-x}Sr_xMnO₃," *Appl. Phys. Lett.* **102**, 071605 (2013).
- ³⁵E. Lesne, N. Reyren, D. Doennig, R. Mattana, H. Jaffrès, V. Cros, F. Petroff, F. Choueikani, P. Ohresser, R. Pentcheva, A. Barthélémy, and M. Bibes, "Suppression of the critical thickness threshold for conductivity at the LaAlO₃/SrTiO₃ interface," *Nat. Commun.* **5**, 4291 (2014).
- ³⁶Y. Zhou, P. Wang, Z. Z. Luan, Y. J. Shi, S. W. Jiang, H. F. Ding, and D. Wu, "Patterning the two dimensional electron gas at the LaAlO₃/SrTiO₃ interface by structured Al capping," *Appl. Phys. Lett.* **110**, 141603 (2017).
- ³⁷D. C. Vaz, E. Lesne, A. Sander, H. Naganuma, E. Jacquet, J. Santamaria, A. Barthélémy, and M. Bibes, "Tuning up or down the critical thickness in LaAlO₃/SrTiO₃ through *in situ* deposition of metal overlayers," *Adv. Mater.* **29**, 1700486 (2017).
- ³⁸Y. W. Xie, Y. Hikita, C. Bell, and H. Y. Hwang, "Control of electronic conduction at an oxide heterointerface using surface polar adsorbates," *Nat. Commun.* **2**, 494 (2011).
- ³⁹K. A. Brown, S. He, D. J. Eichelsdoerfer, M. C. Huang, I. Levy, H. Lee, S. Ryu, P. Irvin, J. Mendez-Arroyo, C. B. Eom, C. A. Mirkin, and J. Levy, "Giant conductivity switching of LaAlO₃/SrTiO₃ heterointerfaces governed by surface protonation," *Nat. Commun.* **7**, 10681 (2016).
- ⁴⁰H. Wang, C. H. Chan, C. H. Suen, S. P. Lau, and J.-Y. Dai, "Magnetotransport properties of layered topological material ZrTe₂ thin film," *ACS Nano* **13**, 6008–6016 (2019).
- ⁴¹B. Zhang, Z. Muhammad, P. Wang, S. Cui, Y. Li, S. Wang, Y. Wu, Z. Liu, H. Zhu, Y. Liu, G. Zhang, D. Liu, L. Song, and Z. Sun, "Electronic structures of Cr-intercalated ZrTe₂ revealed by angle resolved photoemission spectroscopy," *J. Phys. Chem. C* **124**, 16561–16567 (2020).
- ⁴²Z. Muhammad, B. Zhang, H. Lv, H. Shan, Z. Rehman, S. Chen, Z. Sun, X. Wu, A. Zhao, and L. Song, "Transition from semimetal to semiconductor in ZrTe₂ induced by Se substitution," *ACS Nano* **14**, 835–841 (2020).
- ⁴³M. Ren, S. Han, J. Fan, S. Li, S. Wang, F. Zheng, P. Zhang, X. Ma, Q. K. Xue, and C. Song, "Semiconductor-metal phase transition and emergent charge density waves in 1T-ZrX₂ (X = Se, Te)," *arXiv:2102.07915* (2021).
- ⁴⁴B. Leikert, J. Gabel, M. Schmitt, M. Stübinger, P. Scheiderer, L. Veyrat, T.-L. Lee, M. Sing, and R. Claessen, "Controlling the electronic interface properties of AlO_x/SrTiO₃ heterostructures," *Phys. Rev. Mater.* **5**, 065003 (2021).